

Experimental

Angle-resolved supersonic molecular beam scattering (MBS) and Time-of-Flight (TOF) analysis are ideal tools to study the dynamics of gas-surface interactions, such as the direct-inelastic scattering and the trapping-desorption. The dynamics of the direct-inelastic scattering and trapping-desorption can be systematically investigated as a function of incident translational energy (E_{inc}), incident angle(θ_i), detection angle (θ_f) and surface temperature(T_s).

When the incident molecules hit a surface, an important fraction of molecules will reflect back to the gas phase by direct-inelastic scattering with essentially zero residence time on the surface. These molecules retain some of their initial translational energy and momentum information, but part of their translational energy can be dissipated into a surface.

The angle- and velocity- resolved measurements of the direct-inelastic scattering can provide information about the dynamics of energy accommodation.

In a highly corrugated surface, such as etched GaAs, the nonconservation of parallel momentum will play a dominant role in the dynamics of reactive gas-surface scattering.

The incident molecules also can be trapped on a surface if the molecules lose enough kinetic energy and these molecules have a finite probability of thermal desorption.

The angular distribution of the desorbed molecules exhibits a $\cos^n(\theta_f)$ dependence (θ_f is the detection angle and n is the energy scaling number mainly ranging from ~ 0.1 to ~ 20), which can be used to study the trapping-desorption characteristic and distinguish between molecules that have undergone direct-inelastic scattering and trapping-desorption.

In the experiments here, we carried out a pulsed supersonic molecular beam scattering study of the direct-inelastic scattering and trapping-desorption for $\text{Br}_2 + \text{GaAs}(100)$ at room temperature. We have measured TOF spectra of scattered Br_2 from $\text{GaAs}(100)$ surface as a function of incident translational energy (E_{inc}), incident angle (θ_i) and detection angles(θ_f). The TOF distributions show clearly bimodel consisting of direct-inelastic and trapping-desorption components.

A supersonic molecular beam pulse ($\sim 150 \mu\text{s}$) is produced from a piezo-electric valve, skimmed and then chopped by a rotating (200 Hz) slotted disc, before passing through a further collimating element, to produce a gas pulse of $\sim 35 \mu\text{s}$ (fwhm) and an angular divergence of $\sim 1.5^\circ$ making a spot size of $\sim 2\text{-}3 \text{ mm}$ diameter on the target. The housing of a pulsed molecular beam can be rotated around the sample in a plane perpendicular to the sample surface. The pulsed gas molecules hit the surface after a flight of 67 mm from the chopping disc and are scattered towards the floating-potential Brink type ioniser followed by a fast pulse-counting channeltron and a quadrupole mass spectrometer (QMS). The ioniser, in a triply differentially pumped liquid nitrogen cooled chamber, is at a distance of 500 mm from the sample surface. Incident and scattered pulsed molecular beam energies are determined from TOF measurements. The TOF spectra were corrected for the ion flight time through the QMS.

Results

Mathematical method for Time-of-Flight waveform analyses

Fig.1(a) illustrates typical number density TOF spectrum of scattered Br_2 from GaAs(100) surface at 25°C for an incident translational energy $E_{\text{inc}} = 85.45 \text{ kJmol}^{-1}$ at an incident angle, $\theta_i = 80^\circ$, and detection angle, $\theta_f = 60^\circ$. This TOF spectrum displays clearly that it is composed of a narrower fast peak that is superimposed on the leading edge of the second slower and broader peak. The fast narrow peak can be assigned to the direct-inelastic scattering. In contrast, the slow broader peak which fully trapped onto the surface and subsequently desorbs is assigned to the trapping-desorption.

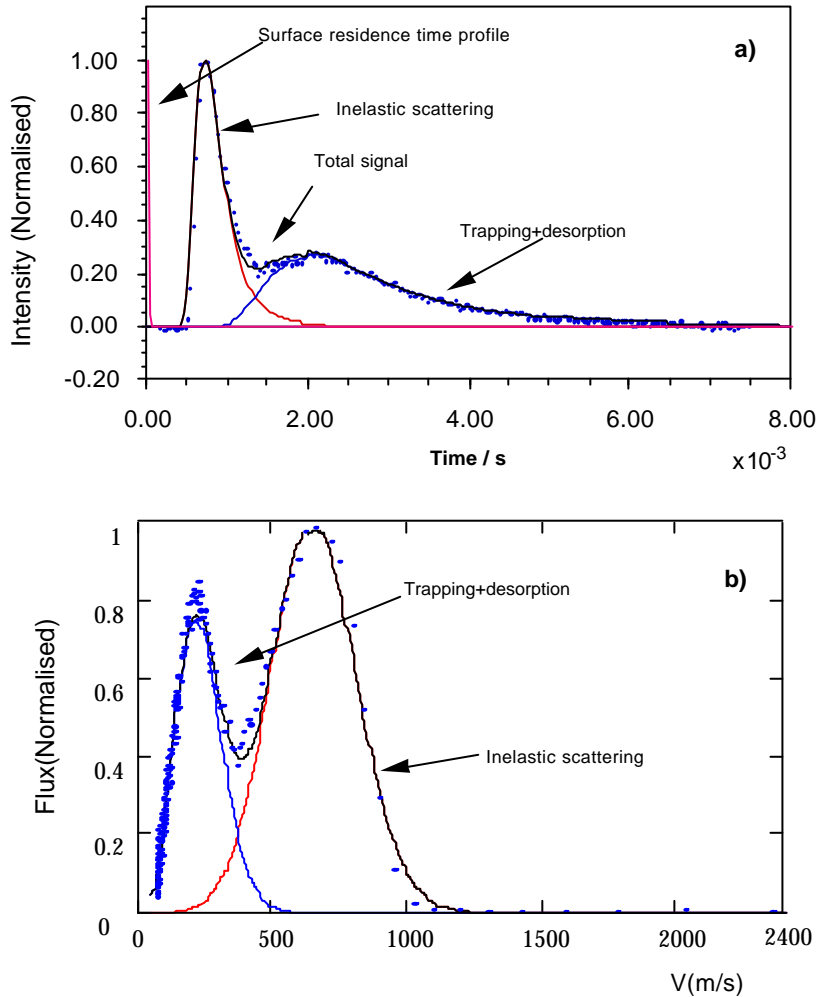


Fig.1 a), TOF intensity distribution of Br_2 scattered from GaAs(100) surface. The lines are backfits to Eq(2). b), Velocity flux distribution of Br_2 converted from the same TOF intensity distribution from a). The lines are backfits to Eq(3). The experimental conditions: $E_{\text{inc}} = 85.45 \text{ kJ/mol}$, $\theta_i = 80^\circ$, $\theta_f = 60^\circ$, $T_s = 25^\circ\text{C}$.

The contribution from the direct-inelastic and trapping-desorption components can be found by fitting the observed TOF waveform to a two component model, made up from a modified gaussian and a Maxwell-Boltzmann distribution at the surface temperature T_s :

$$F(v, v_i) = A \left(F_{di}(v, v_i) + B F_{td}(v) \right) \quad (57)$$

Where $F_{di}(v, v_i)$ and $F_{td}(v)$ are the flux of direct-inelastic scattering and trapping-desorption components; A and B are weights for the total and trapping-desorption fluxes, respectively. v_i indicates the direct-inelastic peak position. Converting Eq (57) to number density and time:

$$T(t) = A \left[\frac{s^3}{t^4} \exp \left[- \left(\frac{s}{\alpha} \left(\frac{1}{t} - \frac{1}{t_i} \right) \right)^2 \right] + B \left(\int_0^t \exp \left(- \frac{t_d}{\tau_d} \right) T_{MB}(t - t_d) dt_d \right) \right] \quad (58)$$

where s is the flight distance and α is the width of the direct-inelastic peak and τ_d is the surface residence time of trapping-desorption species on the surface which we will describe details later in this paper. Eq(58) is true providing that the gas pulse can be treated as a δ function, which can be met in our experimental conditions. At short surface residence times, the measured TOF of trapping-desorption component approaches closely to that expected from a Maxwell-Boltzmann distribution at the surface temperature $T_{MB}(t)$. At long surface residence times, the TOF of trapping-desorption deviates from a Maxwell-Boltzmann distribution with a shift of the peak and long tail.

The lines in Fig.1(a) are least-squares best fits to Eq.(58). In order to obtain angular distributions, the flux of the scattered Br_2 is needed. The intensity-time (number density) frame has to be changed to flux-velocity frame. The following equation was used to transfer from intensity-time distribution to flux-velocity distribution:

$$F(v) = T \left(\frac{s}{v} \right) \frac{s}{v} \quad (59)$$

Fig.1(b) displays the velocity-flux distribution transferred from its TOF number density distribution(Fig.1(a)). Integration of the two peaks in Eq. (59) provides the relative contributions of the direct-inelastic scattering and trapping-desorption components to the total observed signals. The ratio of the trapping-desorption part to the total signals can be used as relative trapping-desorption probability.

Incident translational energy dependence

Fig.2 shows the number intensity TOF distributions of scattered Br_2 from GaAs(100) at the incident angle $\theta_i = 80^\circ$, detection angle $\theta_f = 60^\circ$ for various initial translational

energies (E_{inc}). All the measured number density distributions of Br_2 molecules arriving at QMS are normalised and GaAs(100) surface temperature was 25°C. The direct-inelastic components increase with the initial translational energy. The solid lines through the data represent the sum of the direct-inelastic and trapping-desorption components. The trapping-desorption part was fitted to Maxwell-Boltzmann distributions with its surface residence time applied. The increase of the ratio of the direct-inelastic component to the trapping-desorption means that a molecule is less likely to be trapped on the surface when the initial translational energy increases.

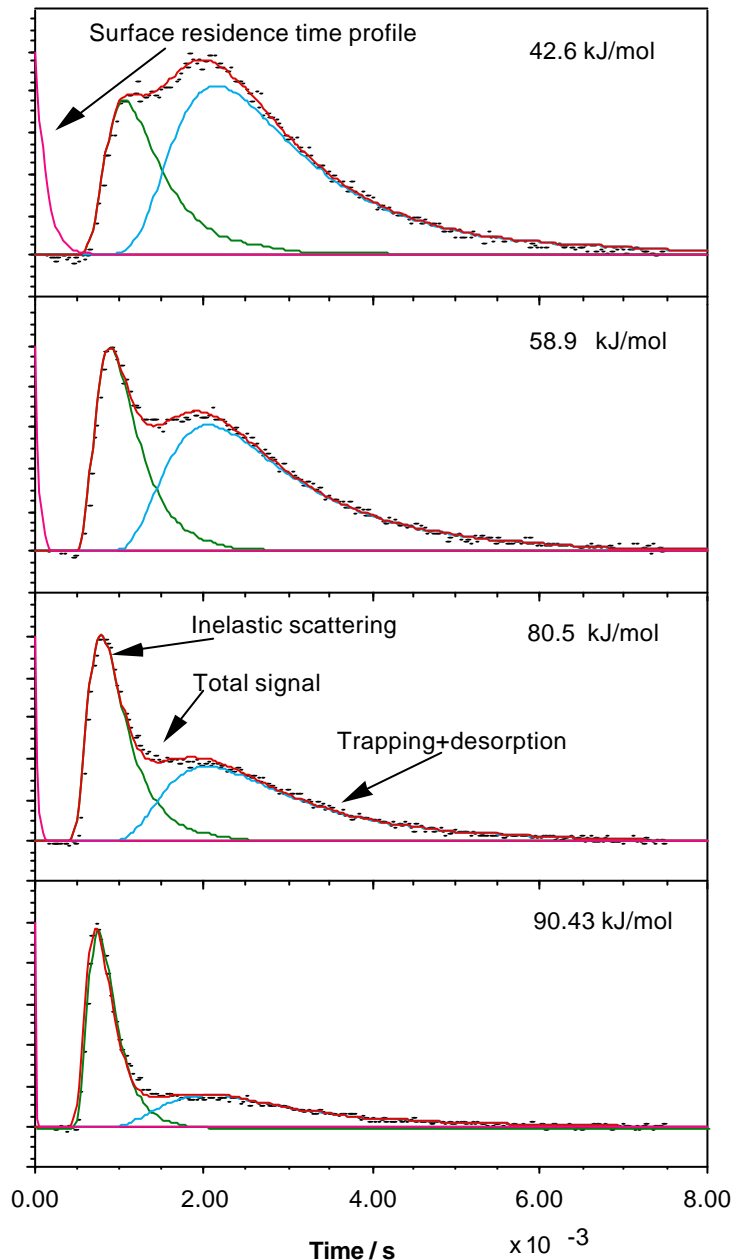


Fig.2 TOF spectra of Br_2 scattered from GaAs(100) surface at temperature of 25°C for various incident translational energies. The incident angle was 80°, the detection angle was 60°.

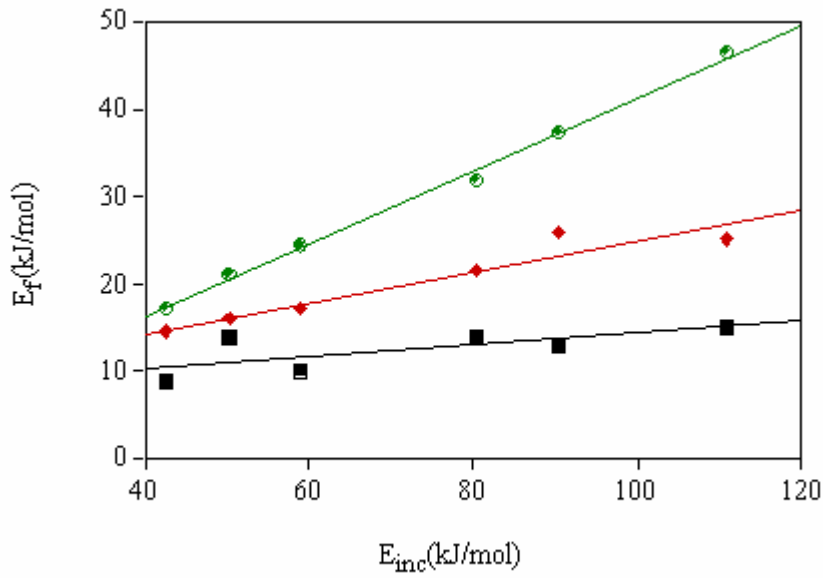


Fig.3. The final output translational energy E_f of the direct-inelastically scattered Br_2 from GaAs (100) surface at temperature of 25 ° C for their various initial incident translational energy E_{inc} . The detection angle was 60°. The filled circles, diamonds and squares represent the incident angles of 80°, 60° and 30°, respectively.

Fig.3 illustrates the final exit average translational energy (E_f) of direct-inelastic scattering of Br_2 with the initial incident translational energy (E_{inc}) at incident angles of 30°, 60° and 80°. Two main features can be observed in this graph: 1) E_f increases with increase of incident translational energy (E_{inc}). The correlation between E_f and E_{inc} displays a good linear relationship at fixed incident and detection angle. 2) E_f and the change of E_f respect to E_{inc} increase with increase of incident angle. A larger fraction of E_{inc} is exchanged at more normal angles of incidence. This behaviour was attributed to more efficient coupling of translational energy to surface phonon as incident angle is more normal to the surface. For a conditions of $E_{inc}=110.9$ kJ/mol, $\theta_f=60^\circ$ and GaAs(100) surface temperature at 25°C, about 42% of the incident energy of Br_2 transfers into a direct-inelastic energy at $\theta_i=80^\circ$, but only 13.7% of E_{inc} transfers to E_f at $\theta_i=30^\circ$.

Polar angular distribution

The polar angular distributions of the total counts, direct-inelastic scattering and trapping-desorption of Br_2 for $\theta_i=30^\circ$, $\theta_i=60^\circ$ and $\theta_i=80^\circ$ have also been shown in Fig.6.

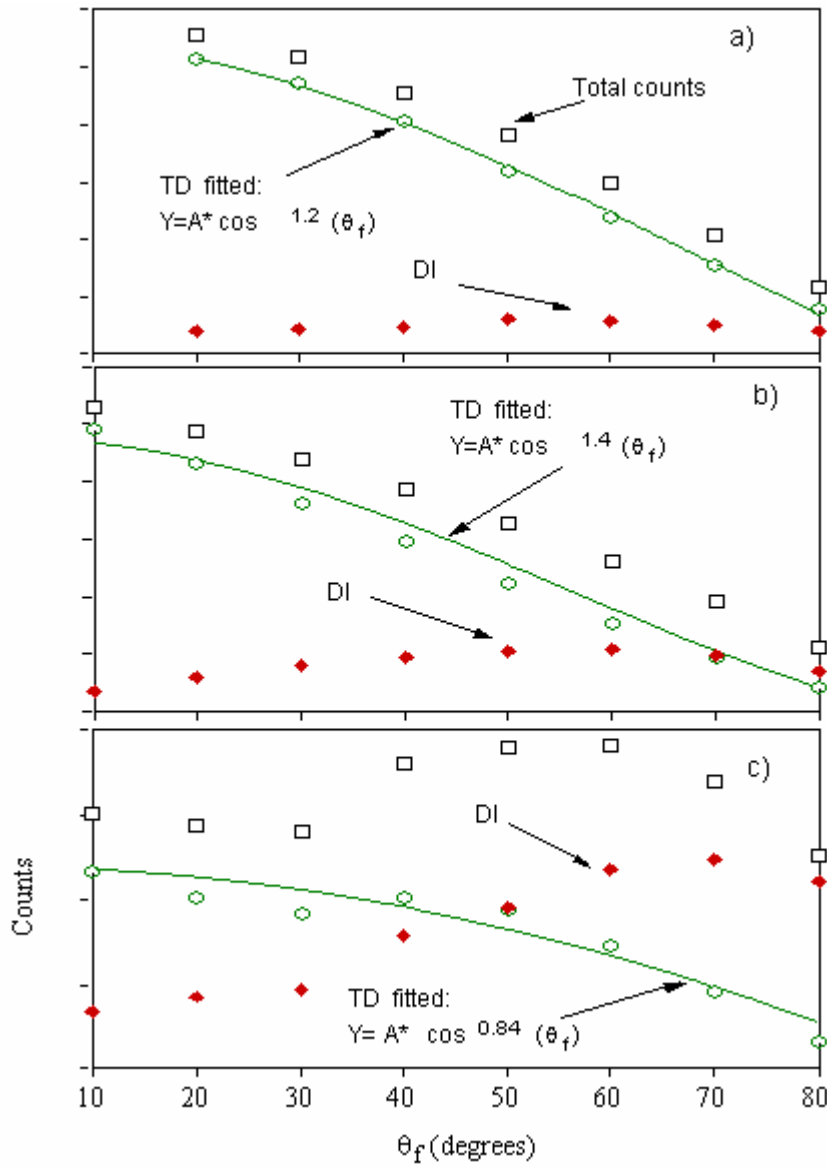


Fig 6. The number density angular distributions of Br_2 at $T_s=25^\circ\text{C}$ of the total, trapping desorption (TD) and direct-inelastic (DI) for a) $\theta_i=30^\circ$, b) $\theta_i=60^\circ$ and c) $\theta_i=80^\circ$ to the surface normal, respectively, with $E_{\text{inc}}=91.45\text{ kJ/mol}$

From Fig.6 we found that all polar angular distributions of the trapping-desorption are close to cosine distribution. The angular distributions of the direct-inelastic scattering are close to their specular angles. Fig.7 shows the angular distributions of Br_2 for three different incident translational energies (42.34, 60.24, and 91.45 kJ/mol, respectively) at $\theta_i=60^\circ$.

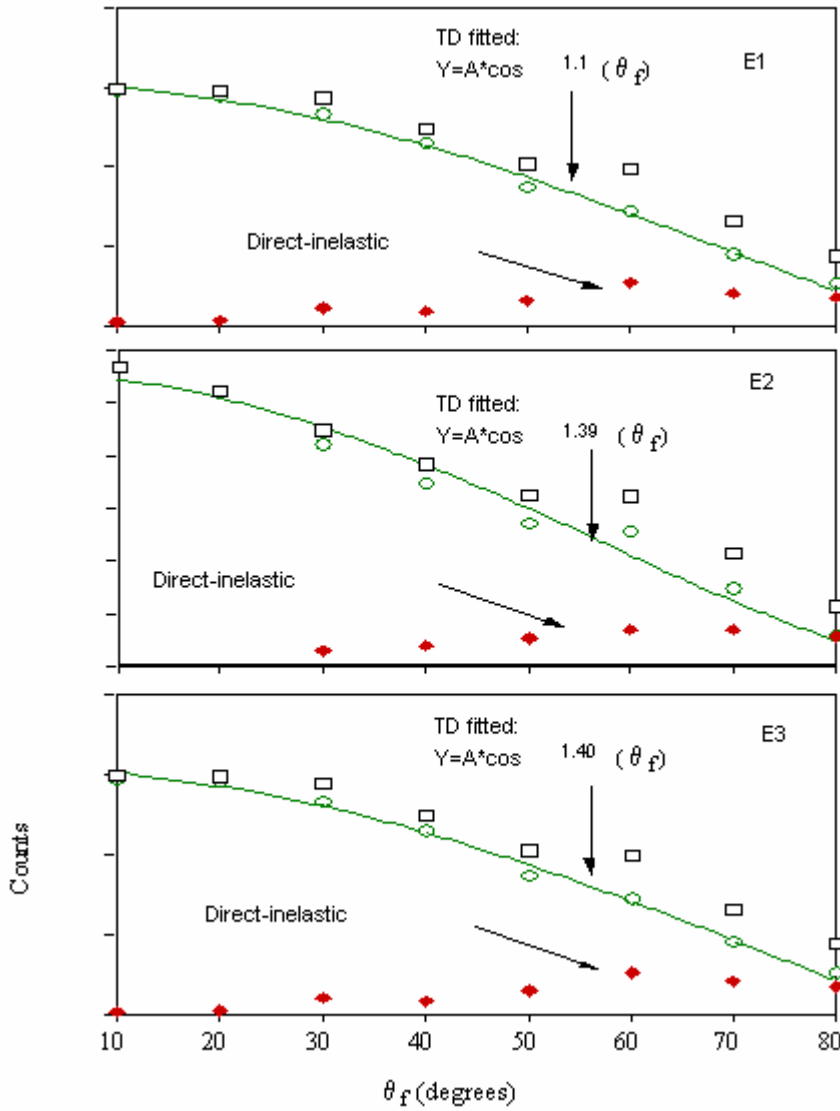


Fig 7. The angular distributions of Br₂ for the three different initial translational energies, $E_1=42.34$ kJ/mol, $E_2=60.24$ kJ/mol and $E_3=91.45$ kJ/mol. $\theta_i=25^\circ\text{C}$. The squares are total intensity, the circles and filled diamonds are the trapping-desorption and direct-inelastic scattering, respectively.

It clearly shows that all the direct-inelastic components peaked near the specular angle although the E_{inc} has been changed from 42.34 kJ/mol to 91.45 kJ/mol. The trapping-desorption components are near cosine distribution, which represents a Maxwell-Boltzmann behaviour. From these angular distribution, it clearly indicates that E_{inc} has very little affect on the trapping-desorption and direct-inelastic scattering features. These results show that trapping-desorption components follows Knudsen law with cosine distribution, independent of θ_i and E_{inc} , while direct-inelastic scattering is isotropic, depends on the incident angle and a maximum peak is near its specular angle.

Incident angle distribution

The initial incident translational energy can be divided into perpendicular energy (also called normal energy: $E_{inc}\cos^2(\theta_i)$) and parallel energy ($E_{inc}\sin^2(\theta_i)$). By change of incident angle, we can examine which part of incident momentum will have more influence on scattering features.

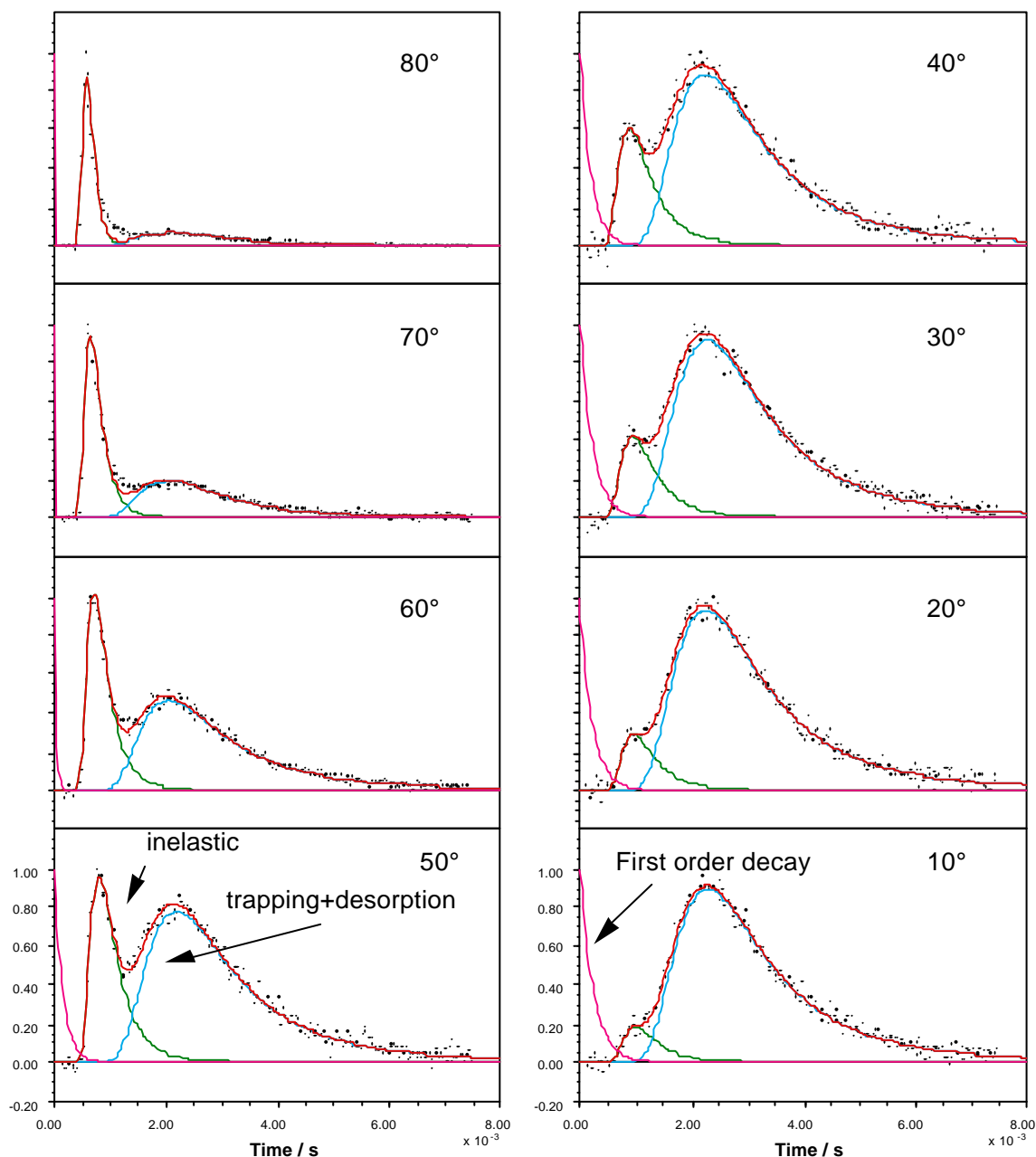


Fig.8 TOF distribution of inelastic and trapping+desorption scattering of Br_2 with various incident angles. The detection angle was 80° ; the initial translational energy of the supersonic molecular beam of Br_2 was 91.45 kJ/mol and the GaAs(100) surface temperature was 25°C .

Fig8. shows TOF intensity distributions of various incident angle for $E_{\text{inc}} = 91.45$ kJ/mol, $\theta_f = 80^\circ$, and $T_s = 25^\circ\text{C}$. As θ_i decrease, the direct-inelastic component falls off, and trapping-desorption component arises.

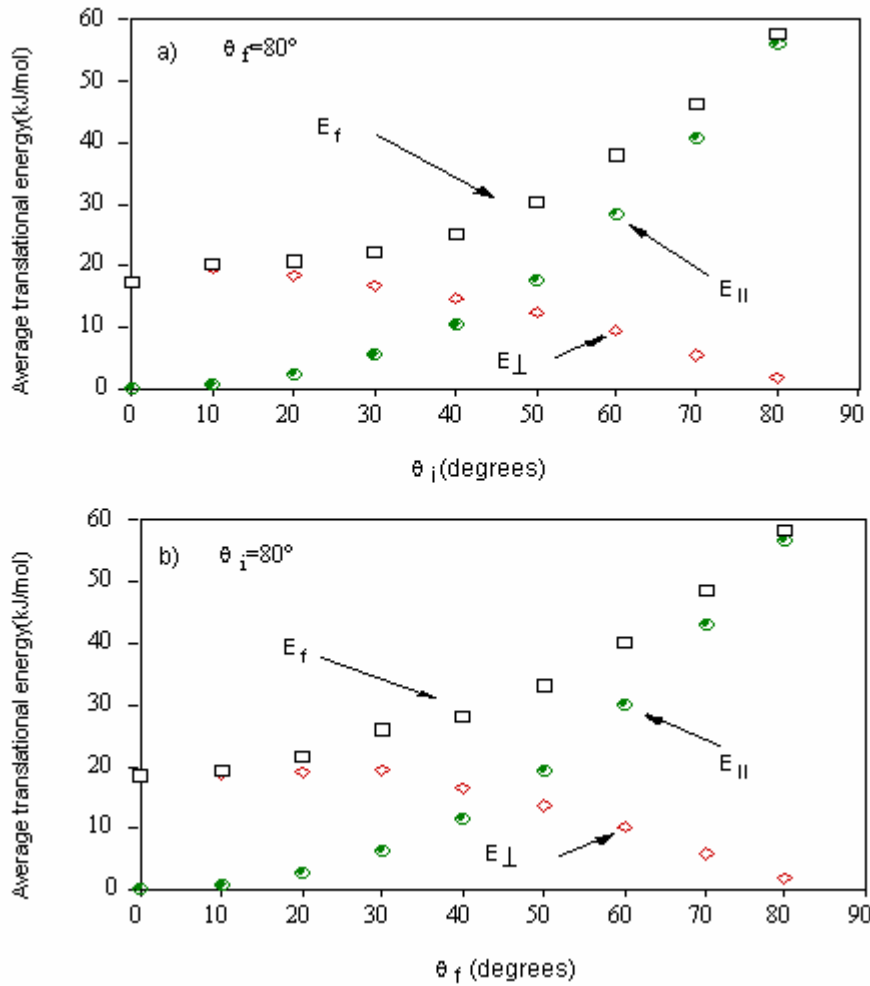


Fig 10 Comparison of the angular dependence of the output energy (final, perpendicular and parallel) of inelastically scattered Br_2 for a) the fixed detection angle $\theta_f = 80^\circ$ and b) the fixed incident angle $\theta_i = 80^\circ$. The initial translational energy was 91.45 kJ/mol and the surface temperature was 25°C

Fig.10 shows two important features: 1) incident and detection angular dependence of E_f , E_{\perp} and E_{\parallel} are same. 2), At small angles (θ_i or $\theta_f < 30^\circ$), E_f change is very small and is mainly attributed to the perpendicular energy(E_{\perp}). At large angle (θ_i or $\theta_f > 40^\circ$), the total output energy increase dramatically, in which E_f was mainly attributed to E_{\parallel} .